Desalination and Water Treatment
www.deswater.com

doi: 10.5004/dwt.2019.23732

151 (2019) 47–55
May

Study on heat and mass transfer characteristics of AGDD

Ping Wang, Bingchen Yu, Shiming Xu*, Lin Xu, Shuping Zhang, Lei Li

Key Laboratory of Ocean Energy Utilization and Energy Conservation of Ministry of Education, School of Energy and Power Engineering, Dalian University of Technology, Dalian 116024, China, Tel. +8613050539216; email: xsming@dlut.edu.cn (S. Xu), Tel. +8613050546586; email: wp2006@dlut.edu.cn (P. Wang), Tel. +8618624287889; email: ybc_chengcheng@163.com (B. Yu), Tel. +8618641505707; email: linlin19872008@126.com (L. Xu), Tel. +8618342245529; email: 2506033595@qq.com (S. Zhang), Tel. +8618041165581; email: lileistu@163.com (L. Li)

Received 23 May 2018; Accepted 30 December 2018

ABSTRACT

The problem of water scarcity becomes an important issue that limits the development of human society. The article studied the air-gap diffusion desalination (AGDD) technology, according to the laws of heat and mass conservation, established a physical and mathematical model for seawater desalination process, and analyzed the sensitivity of hot fluid temperature, cold fluid temperature, fluid flow rate, solution concentration, air-gap width, and model height. The calculation results show that increasing the hot fluid temperature, the cold fluid temperature, reducing the fluid flow rate, air-gap width, and the solution concentration, increasing the model height are all beneficial to improve the efficiency of the device; but increasing the model height reduces the water production per unit area. The results of simulation have an important guiding role on the design of the model size and operating conditions. And the result shows that AGDD has a high GOR (gain output ratio)than AGMD (air gap membrane distillation).

Keywords: Desalination; Diffusion; Heat and mass transfer; Air-gap; Simulation

1. Introduction

Adequate and safe water resources are an important guarantee for the development of human society. And freshwater resources play an important role in modern society. Although, about 70% of the earth's surface is covered by water, only 2.5% of all water resources are freshwater. And icebergs and glacial water account for 77.2% among all freshwater resources, the freshwater resources that can be used directly by people account for only a small part. Desalination is an effective method to solve the problem of water shortage. Air-gap diffusion seawater desalination was simulated in this study, and the sensitivity of the single-stage separation process was analyzed by establishing mathematical model. And the effect of operating parameters and model size in seawater desalination device was obtained.

There are many similarities among the AGDD, the AGMD and the solar-driven diffusion distiller, the latter two seawater desalination processes have been studied in detail. Tanaka [1,2] carried out theoretical and experimental research on the diffusion distiller. He simulated the operation at vernal equinox, summer solstice and winter solstice in the 33°N latitude. The conclusion showed that the output of the desalination process can reach 19.2, 16.0 and 15.9 kg/(m^{2}d) respectively. Tanaka et al., [3] simulated the combined process of single-effect diffusion distillation and inclined capillary distillation under natural conditions, the results showed that the amount of distillation relates to the amount of radiation that input to the distiller. Rajaseenivasan et al., [4] studied the multi-effect solar distillation process and pointed out: increasing the area of the collector or using a parabolic collector can increase the yield; increasing the condensing area can increase the condensation rate and evaporation rate. Reddy et al., [5] pointed out: the concentration and the flow rate of brine play an important role in reducing the production cost of freshwater. Kaushal et al.,

* Corresponding author.

[6] found that after using reheat and reducing the heat loss on the ground and side can improve the performance of the distiller at night. Alkhudhiri et al., [7,8] studied the effects of high-concentration solutions on the diffusion flux and rejection factor of air-gap membrane distillation. The results showed that the decrease in diffusion flux is greater than the decrease of partial pressure of vapor, and the energy consumed increases with the increase in concentration. Li et al., [9] studied direct contact membrane distillation and showed: The difference in the sensitivity of the several solutions to the concentration is due to the difference in activities. When the concentration is high, the increase in viscosity causes the polarization of the temperature, which decreases the diffusion flux, therefore, the effect of viscosity cannot be ignored. Eykens et al., [10], Attia et al., [11] and Khalifa [12] conducted an experimental comparison of contact membrane distillation and air-gap membrane distillation. The results showed that air-gap membrane distillation has greater diffusion flux and can save more energy.

Leu et al., [13] simulated the heat and mass transfer of liquid film evaporation on a vertical plate covered with porous media. They believed that the amount of latent heat transfer in heat transfer is more than sensible heat transfer, and the smaller porosity and thinner thickness can promote higher interface temperatures and mass concentrations. Ming-Hsyan et al., [14] studied the effect of Darcian resistance on mixed convection when fluid evaporation on porous media, they showed that when the Darcian resistance is small, the buoyancy increases gradually, the overall heat transfer rate is cut off, and the fluid evaporation on the wall increases. Yiotis et al., [15] studied the effect of film flow on the drying of porous media. The results showed that the film flow is the main influencing factor of the drying of porous materials. Shirazian et al., [16] established a 3d model to simulate the transmission of water vapor through the membrane and used finite element method to solve the governing equation, the distribution of concentration, and temperature was obtained. Tang et al., [17] studied the gas-liquid multiphase flow problem in vacuum membrane distillation, in the simulation, the aqueous solution of sodium chloride is considered to be a continuous, incompressible fluid. Wang et al., [18] proposed a flat-plate splitter, a pyramidal splitter, and a dome-shaped splitter in order to make the feed in the cross-flow vacuum membrane distillation uniform and improve the performance, the results showed that the pyramidal splitter and the dome-shaped splitter are better than the flat-plate splitter. Ma [19] designed a new type of solar desalination device based on the seawater desalination device. According to theoretical analysis, the solar seawater desalination efficiency is improved by improving the traditional solar desalination device. Liu et al. [20,21] studied the process of the hollow fiber decompression membrane distillation, analyzed the influence of operating conditions on the distribution of heat and mass parameters. Xu et al., [22] simulated the internal heat and mass transfer process of a new heat recovery plate frame air-gap membrane distillation module, and investigated the internal temperature distribution of the flow field under different feed temperatures, flow rates, and vacuum levels. Janajreh et al., [23] studied AGMD and pointed out that when the feed temperature was raised from 50° to 75°, the yield increased from 3.34 to 15.3 g/m^{2}s, and the diffusion flux increased from 11.5 to 52.7 g/m^{2}s. Mahmoudi et al., [12] and Ali et al., [24] have optimized the membrane distillation process, they found that there is an optimal model length for optimal heat recovery, and the optimal value is related to the ratio of the hot and cold fluid flow, the temperature of the hot fluid, and the brine concentration. Nasr et al., [25] simulated the mass and heat transfer of liquid flow on the vertical wall with porous media. The conclusions indicated that the evaporative heat and mass transfer increase when decrease the porosity or the thickness, increase the flow rate or the inlet temperature or lower the atmospheric pressure.

As a combination of membrane separation technology and traditional distillation technology, membrane distillation has special advantage. However, although membrane distillation has been existed for a long time, it has not been used in industry widely. Its hydrophobic membrane is a major limiting factor and membrane fouling has become an important research topic. In our study, the air-gap diffusion seawater desalination process cancelled the presence of a membrane, the hydrophilic porous medium soak with high-temperature saline water acts as hot channel. Compared with hydrophobic membrane, the hydrophilic porous medium effectively reduces the cost of membrane preparation, cleaning and maintenance, and it's more conducive to heat and mass transfer. At the same time, AGDD retains the advantages of membrane distillation, and has low requirements for heat source temperature, which can be warmed by solar energy, geothermal energy or industrial waste heat. The device operates under atmospheric pressure and is heat insulated from the external environment. Based on mass conservation and heat conservation law, in our study, we analyzed the heat and mass transfer mechanism in the AGDD model, and got the influence of device size and operating conditions on the efficiency of the device by numerical simulation. The results can guide the design of the model size and operating conditions.

2. Physical model

Fig. 1. is a schematic diagram of working medium flow process in AGDD device. The air-gap diffused desalination device is mainly composed of two flat plates placed close and parallel to each other. One of the plates cover with porous media acts as evaporator and another plate acts as condenser in which cold fluid flows. When the device running, cold fluid flows from the bottom up in the condenser, flows out from the top and is then heated by external heat source, then become hot fluid, the hot fluid flows into evaporator and flows from the top to the bottom. Since the temperature in the evaporator is higher than the condenser, the partial pressure of water vapor on the evaporator surface is greater than the condenser. Water vapor evaporates from the evaporator surface and diffuses through the air-gap by the drive of the partial pressure difference of water vapor, then condenses on the condenser surface. The condensed freshwater flows along the condenser plate to the bottom of the device by the action of gravity, and then the freshwater is collected. Heat (Q) and mass (m) transfer from the evaporator to the condenser through air-gap. When the water evaporates from the evaporator surface, the latent heat is taken away, and the temperature of the hot fluid is lowered. On the condenser surface, latent heat is released to heat the cold fluid in the condenser,

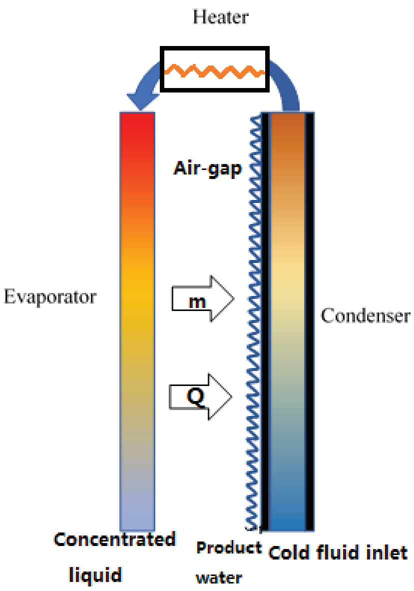

Fig. 1. Schematic diagram of working medium flow process in AGDD device.

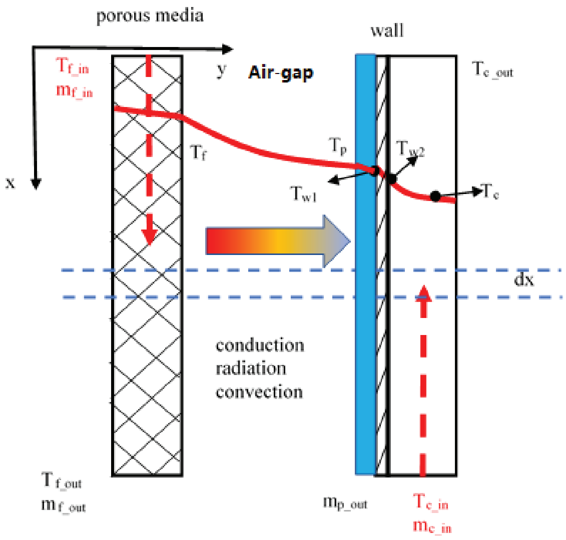

Fig. 2. Air-gap desalination device model.

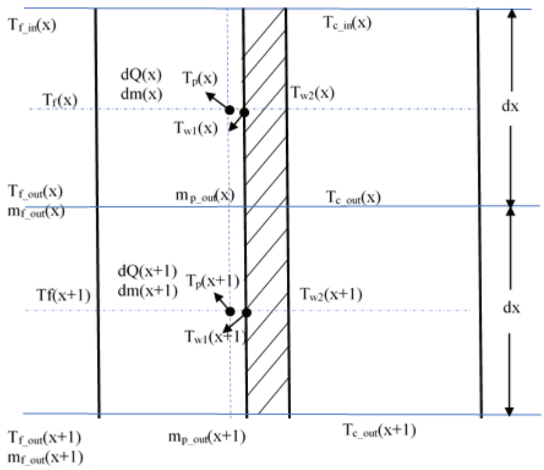

Fig. 3. Slices along the model.

which enables energy recovery. Since the amount of latent heat from vaporization and condensation is approximately the same, the temperature difference between the evaporator and the condenser at the same height is substantially constant. This temperature difference causes the water to evaporate or condense over the entire height. Alsaadi et al., [26] simulated the air-gap membrane distillation in a co-current pattern. The results showed that compared with the countercurrent model, when the height decreases, the diffusion flux in the co-current model decreases rapidly. When the model length is 15 m, the total diffusion of the downstream model is 5% smaller than that of the counter flow model, and the heat of the downstream model cannot be effectively recovered, so the co-current regime isn't studied in our study.

3. Mathematical model

As shown in Fig. 2 and 3, when the device is modeled and analyzed, the x direction is divided into micro cell segments of length dx. In the y direction, heat transfers from the evaporator to the liquid film on the condenser wall in three ways: conduction, radiation, and convection. Then heat transfers to the inner surface of condenser by heat conduction. Finally, the cold fluid absorbs heat by convection. The inlet parameters of evaporator and condenser are known. For mathematical formulation of the problem, the following simplifying assumptions are introduced:

(1) Vapor mixture is an ideal gas;
(2) Flows and transfers in the two phases are steady, laminar;
(3) Air-gap pressure is atmospheric pressure;
(4) The liquid-saturated porous medium is isotropic and homogeneous, Dufour and Soret effects are negligible;
(5) The effect of the superficial tension is negligible. The gas-liquid interface is in thermodynamic equilibrium.

3.1. Mass transfer

Taking the dx element at the x position as the studying object, assuming the upper end is the inlet, the temperature and mass flow rate at the inlet of the evaporator and the condenser are known. According to Fick's law of diffusion, vapor diffusion flux or the flow rate change on the evaporator can be calculated:

$$\frac{dm_f(x)}{dx} = \frac{A}{L}\frac{DP}{R_g Y T_m(x)}\ln\left(\frac{P-P_p(T_p(x))}{P-P_f(T_f(x))}\right) \quad (1)$$

where $T_m(x)$ is the average temperature of evaporator and condenser:

$$T_m(x) = \frac{T_f(x)+T_p(x)}{2} \quad (2)$$

The increase in the flow rate of product water (see Eq. (3)) on the condenser surface is equal to the amount of vapor diffusion.

$$\frac{dm_p(x)}{dx}=\frac{A}{L}\frac{DP}{R_gYT_m(x)}\ln\left(\frac{P-P_p(T_p(x))}{P-P_f(T_f(x))}\right) \quad (3)$$

3.2. Heat transfer

3.2.1. Heat transfer in air-gap

The heat transfer between the evaporator and the condenser is complicated, there are three kinds of heat transfer: conduction, radiation and convection. The air-gap is filled with a mixture of air and water vapor, its thermal conductivity λ_a can be obtained by empirical formula [28], the amount of conductivity $Q_c(x)$ (see Eq. (4)) can be obtained from the Fourier law.

$$Q_c(x)=\frac{\lambda_a A}{L}\frac{T_f(x)-T_p(x)}{Y}dx \quad (4)$$

Taking the elements of evaporator and condenser as two infinite plates, the amount of radiation heat can be calculated as:

$$Q_r(x)=\frac{A}{L}\frac{1}{1/\varepsilon_f+1/\varepsilon_p-1}\sigma(T_f(x)^4-T_p(x)^4)dx \quad (5)$$

It can be seen from Fig. 4. that the $Q_d(x)$ on the evaporator is the sum of latent heat and sensible heat of water vapor at temperature $T_f(x)$.

$$Q_d(x)=dm_f(x)\times h_{\text{vap}}(T_f(x))+dm_f(x)\times h_l(c(x),T_f(x)) \quad (6)$$

Unlike the convective heat transfer on the evaporator, $Q_{\text{cond}}(x)$ is the sum of latent heat released and the sensible heat released when the vapor is cooled from $T_f(x)$ to $T_p(x)$.

$$Q_{\text{cond}}(x)=dm_p(x)\times\int_{T_p(x)}^{T_f(x)}c_{pv}dT+dm_p(x)\times h_{\text{vap}}(T_p(x)) \quad (7)$$

For the evaporator, according to conservation of energy, the enthalpy change of the hot fluid is the sum of the convection $Q_d(x)$, conduction $Q_c(x)$ and radiation $Q_r(x)$. In addition to heat conduction, radiation and convection, the heat input to the condenser also includes the heat $Q_{pl}(x)$ from the upstream high-temperature condensed water.

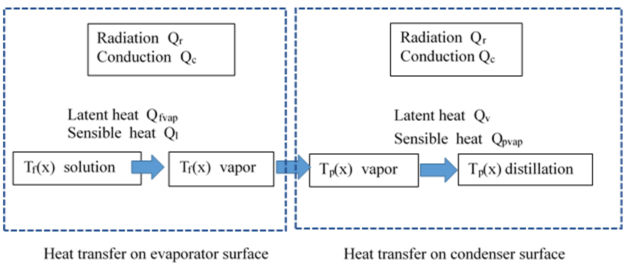

Fig. 4. Diagram of heat transfer in air-gap.

$$d[m_f(x)h_l(c(x),T_f(x))]=Q_d(x)+Q_c(x)+Q_r(x) \quad (8)$$

$$Q_{pl}(x)=m_p(x-1)\int_{T_p(x-1)}^{T_p(x)}c_{pw}dT \quad (9)$$

3.2.2. Heat transfer through the water film and wall of condenser

The heat input to the condenser passes through the liquid film and the wall of condenser. The thickness of the condensate film is related to the amount of condensation, and can be calculated by Eq. (10).

$$\delta=\left(\frac{3\mu_p\int_0^x J_v\cdot dx}{g\rho_p^2}\right)^{1/3} \quad (10)$$

According to the law of energy conservation, Eqs. (11) and (12) can be obtained:

$$Q_{\text{cond}}(x)+Q_c(x)+Q_r(x)+Q_{pl}(x)=\frac{A\lambda_p}{L}\frac{T_p(x)-T_{w1}(x)}{\delta}dx \quad (11)$$

$$\frac{A\lambda_p}{L}\frac{T_p(x)-T_{w1}(x)}{\delta}dx=\frac{A\lambda_w}{L}\frac{T_{w1}(x)-T_{w2}(x)}{d_w}dx \quad (12)$$

3.2.3. Heat transfer between condenser wall and cold fluid

Heat transfers from the inner wall of the condenser to the cold fluid by convection, the $h_w(x)$ is the convection heat transfer coefficient on the inner wall of condenser, the $h_w(x)$ can be calculated by the following formula [28]:

$$\frac{A\lambda_w}{L}\frac{T_{w1}(x)-T_{w2}(x)}{d_w}dx=h_w(x)\frac{A}{L}(T_{w2}(x)-T_c(x))dx \quad (13)$$

3.2.4. Heat absorbed by cold fluid

The cold fluid in the condenser absorbs the heat from the wall, its temperature increases, and the enthalpy increases.

$$h_w(x)\frac{A}{L}(T_{w2}(x)-T_c(x))dx=d[m_c\times h_l(c,T_c(x))] \quad (14)$$

4. Verification of calculation results

Comparing the simulation results from our study with the experimental results from the air-gap membrane distillation device of Alsaadi [26]. The diffusion flux and air-gap parameters were the same as those of Alsaadi's experiment (hot fluid temperature is 333.15 and 343.15 K), and the results are shown in Fig. 5. When the air-gap width is 5 mm, the average relative error is 3.76%. With the increases of air-gap width, the relative error increases. Since the air-gap width has a great influence on the diffusion flux, and it is difficult to measure the air-gap width accurately in experiments, small differences may cause large errors. Therefore, the simulation accuracy will be different under different air-gap widths. The air-gap width of the model studied in this paper is small and the simulation results agree well with the experimental results and can predict the running performance of the process accurately.

5. Simulation results and analysis

5.1. Effect of fluid temperature

5.1.1. Effect of hot fluid temperature

An important indicator to evaluate the seawater desalination process is the GOR (gain output ratio), which is defined as the ratio of the total freshwater output to the amount of steam consumed by the heater. A model with an air-gap width of 5 mm, NaCl solution (as saltwater or fluid) concentration of 0.62 mol/kg, and the height of 1m was simulated, changing the temperature of the hot and cold fluid and the fluid flow rate to analyze the effect on process efficiency. During the operation, the cold fluid flow rate and the hot fluid flow rate are equal.

$$\mathrm{GOR} = \frac{m_p \Delta h}{Q_{\mathrm{in}}} = \frac{m_p \Delta h}{m_f c_p (T_{f\_\mathrm{in}} - T_{c\_\mathrm{out}})} = R \frac{\Delta h}{c_p (T_{f\_\mathrm{in}} - T_{c\_\mathrm{out}})} \tag{15}$$

In Eq. (15) [30], GOR is proportional to the freshwater output m_p and inversely proportional to (T_{f_in}–T_{c_out}), the cold fluid flow rate m_f. At the flow rate of 0.001kg/s, when the temperature of the hot fluid rises, the slope of GOR (Fig. 6.) becomes smaller; this is because the slope of freshwater production m_p decreases. The cold fluid outlet temperature T_{c_out} is related to the hot fluid temperature T_{f_in}. With the increase of the hot fluid temperature T_{f_in}, the amount of water vapor diffusion increases, the latent heat released to heat the cold fluid increases, and the cold fluid outlet temperature T_{c_out} also increases. And the temperature difference (T_{f_in}–T_{c_out}) depends on which one is increased in a greater extent.

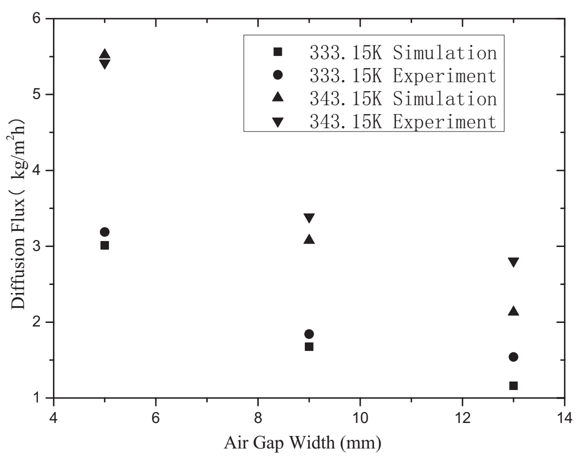

Fig. 5. Comparison between simulation and experiment.

5.1.2. Effect of cold fluid temperature

As shown in Fig. 7, GOR increases with the increase of the cold fluid temperature. As can be seen from Eq. (15), although the increase of cold fluid temperature leads to the decrease of the water vapor diffusion m_p, the main factor that plays a major role in the change of the efficiency value is the required external input heat. The increase of the cold fluid inlet temperature causes the condenser outlet temperature T_{cout} to increase and the amount of heat input from the outside to decrease, so the GOR becomes larger.

5.2. Effect of fluid flow rate

As can be seen from Fig. 8, with the increase of flow rate, the output of freshwater increases and GOR decreases. As the flow rate increases, the temperature of the hot fluid in the evaporator decreases along the x direction slowly,

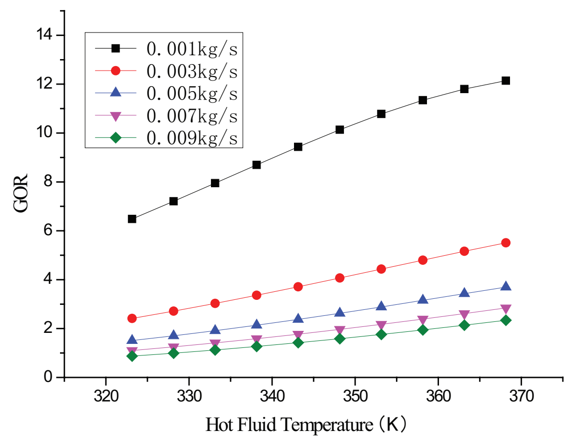

Fig. 6. Effect of hot fluid temperature and flow rate on GOR (concentration 0.62 mol/kg, model height 1m, air-gap width 5 mm, cold fluid temperature 293.15 K).

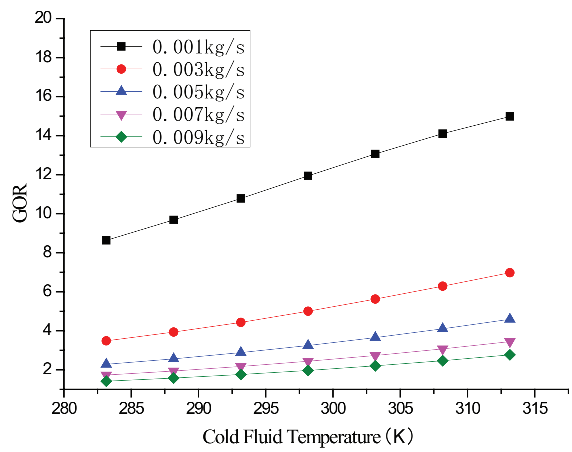

Fig. 7. Effect of cold fluid temperature and flow rate on GOR (concentration 0.62mol/kg, model height 1m, air gap width 5 mm, hot fluid temperature 353.15 K).

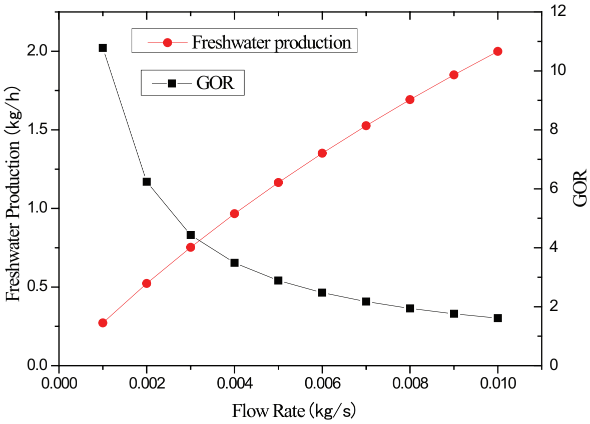

Fig. 8. Effect of flow rate on freshwater yield and GOR (concentration 0.62mol/kg, model height 1m, air-gap width 5 mm, hot fluid temperature 353.15 K, cold fluid temperature 293.15 K).

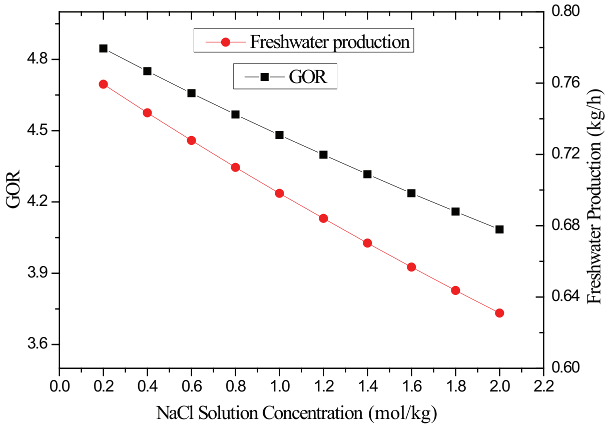

Fig. 9. Effect of NaCl solution concentration on freshwater yield and GOR (flow rate 0.003kg/s, model height 1m, air-gap width 5 mm, hot fluid temperature 353.15 K, cold fluid temperature 293.15 K).

meanwhile, the temperature of the cold fluid in the condenser rises slowly too, the temperature difference of fluid between the evaporator and the condenser increases, and the diffusion flux increases. With the increase of flow rate, the temperature difference (T_{f_in}–T_{c_out}) between the inlet of the evaporator and the outlet of the condenser becomes larger, which requires an increase in external heating. At the same time, the increase in heating does not lead to a sufficient increase in the amount of diffusion, resulting in the GOR of the process reducing. When the flow rate is small, the slope of the GOR line is relatively large, the flow rate has a greater influence on the GOR.

5.3. Effect of NaCl solution concentration

Sensitivity analysis was performed on the NaCl solution concentration and the results are shown in Fig. 9. It can be seen that as the NaCl solution concentration of the solution increases, both the freshwater yield and GOR decrease. As the NaCl solution concentration increases, the vapor pressure on the surface of the evaporator decreases, the driving force of the evaporation diffusion process decreases, so the output of the freshwater decreases;. When the diffusion flux reduced, the heat transfer decreases, the outlet temperature T_{c_out} of condenser decreases, but the inlet temperature T_{f_in} of evaporator does not change, and the amount of heating required from the external heat source is increased, resulting in the decrease in efficiency.

5.4. Effect of the width of air-gap

As Fig. 10, shows: with the air-gap width increases, both the freshwater yield and GOR decreases. As we can see from Eq. (1), vapor diffusion flux is inversely proportional to the air-gap width, so reducing the air-gap width is beneficial to increase the diffusion flux and improve the freshwater yield and GOR. However, when the air-gap width is reduced, it is possible that the hot fluid on the evaporator surface contacts with the freshwater produced on the condenser surface. So during the experiment and the device design, the occurrence of contamination should be avoided.

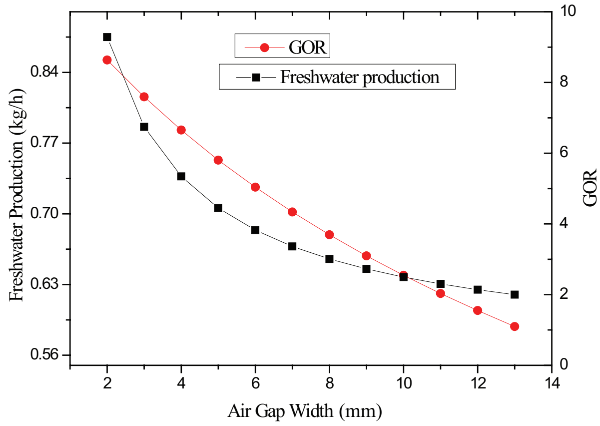

Fig. 10. Effect of air-gap width on freshwater yield and GOR (flow rate 0.003 kg/s, model height 1m, concentration 0.62mol/kg, hot fluid temperature 353.15 K, cold fluid temperature 293.15 K).

5.5. Effect of model height

As shown in Fig. 11, with the height increases, the yield and GOR increase, but the slope of the yield curve gradually decrease, indicating that the increase in model length has a weaker and weaker effect on yield, which can be seen from the influence of the height on the diffusion flux. As the height increases, the freshwater yield per unit area (diffusion flux) decreases. Therefore, when designing the model, we can't increase the yield by increasing the height indefinitely, the cost of equipment investment should also be considered.

5.6. Combined influence of fluid temperature and flow rate on performance

When the air-gap width is 5 mm, the model height is 1 m and the concentration of NaCl solution is 0.62 mol/kg, we studied the effects of hot fluid temperature, cold fluid temperature and flow rate on the working performance of the device.

As we can see from Fig. 12, the yield of freshwater (Fig. 12(a)) and the GOR (Fig. 12(b)) increase with the increase of hot fluid temperature, the driving force of vapor diffusion is the temperature difference between the evaporator and the condenser. When the inlet temperature of the cold fluid

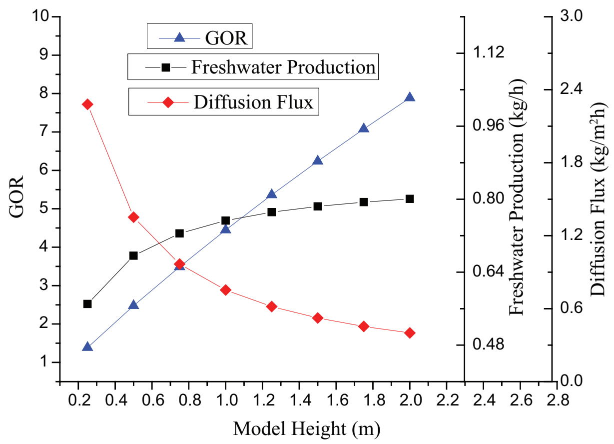

Fig. 11. Effect of model height on yield, GOR, and diffusivity (flow rate 0.003 kg/s, air gap width 5 mm, concentration 0.62 mol/kg, hot fluid temperature 353.15 K, cold fluid temperature 293.15 K).

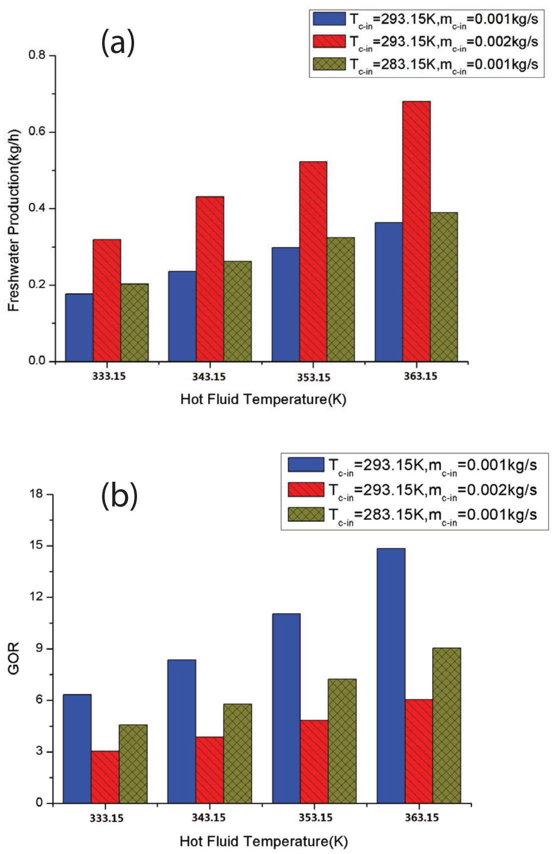

Fig. 12. Effect of cold fluid temperature, hot fluid temperature and flow rate on GOR and freshwater production (concentration 0.62 mol/kg, model height 1 m, air-gap width 5 mm).

remains unchanged, with the temperature of the hot fluid increases, the driving force for vapor diffusion increases, so that the yield of freshwater increases. GOR is proportional to the freshwater production and inversely proportional to the external heating steam quantity. While the temperature of hot fluid rises, the amount of external heating steam in heater increases at a certain temperature of external heat source, however the increase of fresh water production is the main factor, so that the GOR increases with the increase of the hot fluid temperature.

When the flow rate increases, the yield of freshwater increases and GOR decreases. With the flow rate increases, the temperature in the evaporator and condenser changes slowly, the temperature difference between the evaporator and the condenser increases, which encourages the process of diffusion, the temperature difference between the inlet of the evaporator and the outlet of the condenser becomes larger, so the amount of heating from the outside increases and the GOR is reduced.

When the cold fluid temperature increases, GOR increases and the yield of freshwater decreases. This is because increasing the temperature of cold fluids results in decreasing the temperature difference between the evaporator and the condenser, and the water vapor pressure difference is reduced, the diffusion driving force is reduced, and the diffusion flux decreases, and then yield of freshwater decreases. Although the water vapor production is reduced, the increase of the inlet temperature of the cold fluid causes the increase of the outlet temperature of the condenser, and the amount of heating from the outside is reduced, which is the main influence factor, as a result, GOR increases with the increase of the cold fluid temperature.

Considering the combined influence of hot fluid temperature, cold fluid temperature and flow rate on the performance of the device, when the hot fluid temperature higher, the fluid flow rate larger, the cold water temperature lower, the yield of freshwater will be higher; when the hot fluid temperature higher, the flow rate smaller, the cold fluid temperature higher, then the GOR will be larger. As shown in Fig. 12, when the cold fluid temperature is 293.15 K and the flow rate is 0.002kg/s, the slope of the fresh water production curve is larger; when the cold fluid temperature is 293.15 K, and the flow rate is 0.001kg/s, the slope of the GOR curve is larger.

5.7. The comparison between air-gap diffusion and air-gap membrane distillation

Comparing the simulation results from our study with the experimental results from the air-gap membrane distillation device of Yan et al., [30]. When the hot fluid temperature is 53.8°C the cold fluid temperature is 25.6°C, and the feed flow is 20 L/h, and under the same operating costs, the membrane of Yan's experience is 245 × 212 mm, its GOR is 1.13. And our model's length and width are respectively 2m and 1m, the GOR is 2.86 which is 2.53 times than that of his experience, which further shows that porous media is conducive to heat and mass transfer in air-gap diffusion. On the one hand, When porous medium is added to the evaporation, it can cause disturbance, lead to heat dispersion effect, and reduce the thickness of boundary layer, promote evaporate and due to the existence of tortuosity, increase the residence time of fluid in the channel, make the fluid fully heat transfer; On the other hand, the surface of porous media is uneven, and when the fluid flows through its surface, the surface area of evaporation is larger than that of plat. It increases the evaporation of water vapor, thus increasing the output of fresh water.

6. Conclusion

Air-gap diffusion seawater desalination is a new type of seawater desalination method. The device has a large surface area, the operation process does not need vacuum environment and can recycle energy. Compared with AGMD, porous media avoids the problem that the membrane preparation and maintenance is expensive; the GOR of AGDD is 2.53 times than AGMD, which indicates that the porous medium is more conducive to heat and mass transfer, and the fresh water production is higher. So air-gap desalination has a good application prospect. In our study, the physical model of single-stage air-gap desalination is established. Using the established model to simulate the desalination process, the results show that increasing the hot fluid temperature can increase the diffusion flux and the efficiency; increasing the cold fluid temperature can reduce the diffusion flux and increases the efficiency; although increasing the fluid flow rate can increase the diffusion flux, it reduces the efficiency; increasing the concentration of the NaCl solution reduces the vapor pressure on the surface of the evaporator, which adversely affects the separation process; reducing the air-gap width can improve the performance of the device, but small air-gap width may cause the solution in the evaporator to come in contact with the freshwater and cause contamination; increasing the height of the model can increase the yield and the efficiency, but the freshwater production per unit area decreases, and the investment in equipment increases. The device can work by solar energy, geothermal energy or industrial waste heat. When designing the device, the air-gap width should be small as much as possible; the height of the device should be long on the premise of considering the freshwater production per unit area. In the actual operation process, to increase the hot fluid temperature, and decrease the cold fluid temperature, improve the fluid flow rate, may product more freshwater yield.

Symbols

a	Total wall area, m^2
c	Molar concentration, mol/kg
c_p	Constant pressure specific heat of solution, J/kg K
c_{pv}	Constant pressure specific heat of vapor, J/kg K
c_{pw}	Constant pressure specific heat of water, J/kg K
d_w	Wall thickness, m
dx	Microelement length, m
GOR	Gain output ratio
Δh	Heat of unit mass steam, J
h_1	Specific enthalphy of solution, J/kg
h_{vap}	Steam latent heat, J/kg
h_w	Heat transfer coefficient of coolant channel, W/m^2 K
L	Model height, m
M	Molar mass of NaCl, kg/mol
m	Mass flow rate, kg/s
P	Pressure, Pa
Q_c	Thermal conductivity, W
Q_{cond}	Convection heat transfer on condenser, W
Q_d	Convection heat transfer on evaporator, W
Q_{pl}	Heat from upstream on condenser, W
Q_r	Heat radiation, W
R	Recovery rate
R_g	Universal gas constant, J/kg K
R_q	Thermal resistance, K/W
T	Temperature, K
T_w	Temperature of wall of condenser, K
x	Longitudinal coordinate
y	Lateral coordinate
Y	The width of air-gap, m

Greeks

λ_a	Thermal conductivity of wet air, W/m K
λ_c	Thermal conductivity of NaCl solution, W/m K
λ_w	Thermal conductivity of condenser wall, W/m K
ε	Surface emissivity
σ	Black body radiation constant, $W/m^2 K^4$
μ_p	Dynamic viscosity of water, Pa s

Subscripts

in	Inlet
out	Uutlet
m	Average value of the evaporator and the condenser.
f	Hot fluid
p	Product water

Acknowledgement

We are deeply indebted to the National Natural Science Foundation of China (No. 51876023, No.51776029, No.51276029) for its funding, and the Liaoning Province's Natural Foundation Guidance Project (No. 20180550732).

References

[1] H. Tanaka, Theoretical analysis of a vertical multiple-effect diffusion solar still coupled with a tilted wick still, Desalination, 337 (2016) 65–72.
[2] H. Tanaka, Parametric investigation of a vertical multiple-effect diffusion solar still coupled with a tilted wick still, Desalination, 408 (2017) 119–126.
[3] H. Tanaka, K. Iishi, Experimental study of a vertical single-effect diffusion solar still coupled with a tilted wick still, Desalination,402 (2017) 19–24.
[4] T. Rajaseenivasan, K.K. Murugavel, T. Elango, R.S. Hansen, A review of different methods to enhance the productivity of the multi-effect solar still, Renew. Sustain. Energy Rev., 17 (2013) 248–259.
[5] K.S. Reddy, H. Sharon, Active multi-effect vertical solar still: mathematical modeling performance investigation and enviro-economic analyses, Desalination, 395 (2016) 99–120.
[6] A.K. Kaushal, M.K. Mittal, D. Gangacharyulu, An experimental study of floating wick basin type vertical multiple effect diffusion solar still with waste heat recovery, Desalination, 414 (2017) 35–45.
[7] A. Alkhudhiri, N. Hilal, Air gap membrane distillation: a detailed study of high saline solution, Desalination, 403 (2017) 179–186.

[8] A. Alkhudhiri, N. Darwish, N. Hilal, Produced water treatment: application of air gap membrane distillation, Desalination, 309 (2013) 46–51.
[9] J. Li, Y. Guan, F. Cheng, Y. Liu, Treatment of high salinity brines by direct contact membrane distillation: effect of membrane characteristics and salinity, Chemosphere, 140 (2015) 143–149.
[10] L. Eykens, I. Hitsov, K.D. Sitter, C. Dotremont, L. Pinoy, B. Van der Bruggen, Direct contact and air gap membrane distillation: differences and similarities between lab and pilot scale, Desalination, 422 (2017) 91–100.
[11] H. Attia, M.S. Osman, D.J. Johnson, C. Wright, N. Hilal, Modelling of air gap membrane distillation and its application in heavy metals removal, Desalination, 424 (2017) 27–36.
[12] F. Mahmoudi, G.M. Goodarzi, S. Dehghani, A. Akbarzadeh, Experimental and theoretical study of a lab scale permeate gap membrane distillation setup for desalination, Desalination, 419 (2017) 197–210.
[13] J. S. Leu, J.Y. Jang, C. Yin, Heat and mass transfer for liquid film evaporation along a vertical plate covered with a thin porous layer, Int. J. Heat Mass Transfer, 49 (2006) 1937–1945.
[14] S. Ming-Hsyan, M.J. Huang, C.K. Chen, A study of the liquid evaporation with Darcian resistance effect on mixed convection in porous media, Int. Commun. Heat Mass Transfer, 32 (2005) 685–694.
[15] A.G. Yiotis, A.G. Boudouvis, A.K. Stubos, I.N. Tsimpanogiannis, Y.C. Yortsos, Effect of liquid films on the drying of porous media, AIChE J., 50 (2004) 2721–2737.
[16] S. Shirazian, S.N. Ashrafizadeh, 3D modeling and simulation of mass transfer in vapor transport through porous membranes, Chem. Eng. Technol., 36 (2013) 177–185.
[17] N. Tang, H. Zhang, W. Wang, Computational fluid dynamics numerical simulation of vacuum membrane distillation for aqueous NaCl solution, Desalination, 274 (2011) 120–129.
[18] L. Wang, H. Wang, B. Li, Y. Wang, S. Wang, Novel design of liquid distributors for VMD performance improvement based on cross-flow membrane module, Desalination, 336 (2014) 80–86.
[19] L. Ma, Research on solar desalination plant, Chang 'an: Chang 'an University, 2010.
[20] J. Liu, Simulation of the microscopic characteristics of pressure reducing membrane distillation process, Tianjin: Tianjin University, 2015.
[21] J. Liu, B.A. Li, Simulation analysis of thermal mass transfer characteristics of fiber membrane surface in pressure reducing membrane distillation process, Chem. Ind. Eng., 33 (2016) 80–87.
[22] K. Xu, B.A. Li, CFD numerical simulation of flow field in a new plate-frame air gap membrane distillation module, Membr. Sci. Technol., 37 (2017) 88–95.
[23] I. Janajreh, K.E. Kadi, R. Hashaikeh, R. Ahmed, Numerical investigation of air gap membrane distillation (AGMD): seeking optimal performance, Desalination, 424 (2017) 122–130.
[24] A. Ali, J.H. Tsai, K.L. Tung, E. Drioli, F. Macedoni. Designing and optimization of continuous direct contact membrane distillation process, Desalination, 426 (2018) 97–107.
[25] A. Nasr, A.S. Al-Ghamdi, Numerical study of evaporation of falling liquid film on one of two vertical plates covered with a thin porous layer by free convection, Int. J. Thermal Sci., 112 (2017) 335–344.
[26] A.S. Alsaadi, N. Ghaffour, J.D. Li, S. Gray, L. Francis, H. Maab, G.L. Amy, Modeling of air-gap membrane distillation process: a theoretical and experimental study, J. Membr. Sci., 445 (2013) 53–65.
[27] X.H. Wang, M.D. Zhou, H.J. Cheng, Calculation of thermal properties of wet air, The Papers Collection of the Fourth Annual Meeting of National Regional Energy Professional Committee, Engineering Science and Technology II—ArchitecturalScience and Engineering, Mudanjiang: China Society of Architecture Building Thermal Power Branch, (2013) 482–485.
[28] S.G. Lovineh, M. Asghari, B. Rajaei, Numerical simulation and theoretical study on simultaneous effects of operating parameters in vacuum membrane distillation, Desalination, 314 (2013) 59–66.
[29] H. Geng, H. Wu, P. Li, Q. He, Study on a new air-gap membrane distillation module for desalination, Desalination, 334 (2014) 29–38.
[30] J.M. Yan, Q.P. Yuan, R.Y. Ma, Study on the transfer process of air gap membrane distillation, J. Chem. Eng. Chinese Universities, 14 (2000) 109–114.